

1-Methylcyclohexene, methylenecyclohexane, and 1-ethylcyclohexene were samples of >99 mole % purity provided by Dr. Kenneth S. Greenlee of Chemical Samples Co., Columbus, Ohio. 1-Methylcyclopentene ( $n^{20}_D$  1.4320) and 1-isopropylcyclohexene ( $n^{20}_D$  1.4574) were synthesized *via* the Grignard route. The latter olefin contained approximately 8% of the isomeric isopropylidencyclohexane.  $\alpha$ -Pinene ( $n^{20}_D$  1.4660,  $[\alpha]^{20}_D +47.6^\circ$ ) and  $\beta$ -pinene ( $n^{20}_D$  1.4785,  $[\alpha]^{20}_D -21.1^\circ$ ) were obtained from the Glidden Co.

**Hydroboration-Displacement Experiments.** In a typical experiment 9.6 g of 1-methylcyclohexene (100 mmoles) was placed in a three-necked flask fitted with a dropping funnel and a stirring bar, and connected to a Todd microcolumn. To the olefin was added 45 ml of a 1.00 M solution of sodium borohydride in diglyme. The system was flushed and then maintained under a static pressure of nitrogen throughout the hydroboration and displacement stages. Hydroboration was accomplished by adding 16.5 ml of a 3.65 M solution of boron trifluoride in diglyme to the well-stirred reaction mixture. The reaction flask was maintained for 30 min at room temperature.

To the reaction product was added 200 mmoles of 1-decene. The reaction mixture was heated to gentle reflux and the displaced olefin collected in an ice-cooled graduated receiver as the product reached the distillation head. In 6 hr there was collected 8.06 g, a yield of 84%. Gas chromatographic analysis of the product revealed 77% of 1-methylcyclohexene and 23% of 3-methylcyclohexene.

In the above procedure the amount of hydride used was 20% in excess of hydroboration to the dialkylborane stage. Similar amounts of hydride were used for 1-methylcyclopentene and  $\alpha$ -pinene. For cyclopentene, cyclohexene, methylenecyclohexane, norbornene, and  $\beta$ -pinene, which undergo ready hydroboration to the trialkylborane stage, we utilized 30 ml of a 1.00 M solution of sodium borohydride and an equivalent quantity of boron trifluoride.

$\alpha$ - and  $\beta$ -pinene were hydroborated in triglyme solution, using boron trifluoride triglymate. The higher boiling solvent facilitated distillation of these less volatile olefins.

The experimental results from these hydroboration-displacement experiments are reported in Table I.

**Hydroboration-Isomerization-Displacement Experiments.** The following experimental procedure is typical. In a 200-ml flask fitted with a small Vigreux column was placed 11.0 g of 1-ethylcyclohexene (100 mmoles) and 30 ml of a 1.00 M solution of sodium borohydride in diglyme. (Since isomerization proceeds to a trialkylborane derivative, the amount of hydride utilized is based on this conversion). The flask and apparatus was flushed with nitrogen and a static nitrogen pressure was maintained throughout the reaction. Hydroboration was accomplished by adding 11.0 ml

of a 3.65 M solution of boron trifluoride diglymate to the well-stirred reaction mixture at room temperature.

The reaction mixture was heated to reflux (155–160°) and maintained at this temperature for 4 hr. After completion of the isomerization, 200 mmoles of 1-decene was added to the reaction mixture and the heating continued. The displaced olefin was distilled out through the Vigreux column, maintaining the distillation at such a rate as to minimize the amount of diglyme and 1-decene which codistilled.

After 6 hr, the reaction was halted. Gas chromatographic analysis of the distillate indicated a 62% yield of vinylcyclohexane. The olefin mixture was distilled through a Podbielniak 8-mm Heligrig column to obtain pure vinylcyclohexane, bp 124° at 750 mm,  $n^{20}_D$  1.4455.

A slightly modified procedure was utilized for the conversion of  $\alpha$ -pinene to  $\beta$ -pinene. In view of the similarity in the boiling points of  $\beta$ -pinene, diglyme, and 1-decene, the latter substances were substituted by the less volatile triglyme and 1-dodecene. Both the isomerization and the displacement were carried out at 160°, utilizing reduced pressure to remove the  $\beta$ -pinene displaced. Gas chromatographic analysis indicated a 71% yield of  $\beta$ -pinene. Preparative gas chromatography was utilized to separate the  $\beta$ -pinene from the minor amounts of  $\alpha$ - and  $\delta$ -pinene present in the product. The  $\beta$ -pinene thus obtained exhibited  $n^{20}_D$  1.4789,  $[\alpha]^{20}_D -20.6^\circ$ . Thus the  $\beta$ -pinene had undergone the isomerization without detectable racemization.

The results of these experiments are summarized in Table III.

**Rates of Displacement of  $\beta$ -Pinene.** In a 100-ml flask was placed 6.8 g of  $\beta$ -pinene (50 mmoles) and 15 ml of a 1.00 M solution of sodium borohydride in diglyme. After hydroboration was accomplished with 5.5 ml of 3.65 M boron trifluoride in diglyme, there was added 11.2 g of 1-octene (100 mmoles) and 4.08 g of *n*-nonane (internal standard). The flask was heated to  $140 \pm 5^\circ$ . Samples were withdrawn at different time intervals and oxidized with alkaline hydrogen peroxide to destroy the organoborane. The mixture was extracted with ether; the latter was dried over anhydrous magnesium sulfate and then analyzed by glpc using the *n*-nonane as reference.

In a second experiment,  $\beta$ -pinene was hydroborated in an identical manner and the *cis*-myrtanyl derivative isomerized to the *trans* by heating at 160° for 2 hr. 1-Octene was then added and the displacement at 145° followed as described above.

In a third experiment,  $\alpha$ -pinene was hydroborated and the isopinocampheylborane isomerized for 2 hr at 160°. Then 1-octene was added and the displacement with time at 145° followed as in the related two experiments.

The experimental results are shown graphically in Figure 1.

## Electron Spin Resonance Spectra of Low Molecular Weight and High Molecular Weight Peroxy Radicals

James C. W. Chien and C. R. Boss

Contribution from the Research Center, Hercules Inc.,  
Wilmington, Delaware 19899. Received October 7, 1966

**Abstract:** The electron spin resonance (esr) spectra of *t*-butyl, cumyl, polyethylene, polypropylene, and squalane peroxy radicals have been obtained. The temperatures at which various group and molecular averaging processes become important have been determined. The mobility of hindered phenol additives in polypropylene is reflected by the residual dipolar coupling in the esr spectra of the phenoxy radicals.

In the kinetic study of autoxidation of polypropylene by esr,<sup>1</sup> there were two problems of concern: the identity and the mobility of the radicals. The esr spectra of the propagating radicals change both in line shape and line width with temperature. Three radical

intermediates are often postulated in an autoxidizing system: R·, RO·, and RO<sub>2</sub>·. Presumably, R·, which combines with O<sub>2</sub> with diffusion-limited rates under these conditions,<sup>2</sup> is not present in amounts to be detected. Though earlier reports<sup>3</sup> of detection of RO·

(1) J. C. W. Chien and C. R. Boss, Submitted for publication.

(2) L. Bateman, *Quart. Rev.* (London), **8**, 147 (1954).

(3) L. H. Piette and W. C. Landgraf, *J. Chem. Phys.*, **32**, 1107 (1960).

radicals by esr have been disclaimed,<sup>4,5</sup> their presence in appreciable amounts remains a possibility. The most probable of the three radical species is  $\text{RO}_2\cdot$ . The identification of the radical in an autoxidation reaction is of considerable interest.

In considerations of the intra- vs. intermolecular processes in autoxidation,<sup>6</sup> the mobility of the propagating radicals is of consequence. When inhibitor is introduced into a system, its mobility would be reflected by its effectiveness as an antioxidant. A study of relaxation mechanisms and molecular averaging processes by esr should increase our understanding of these questions.

The systems chosen in this investigation allow us to observe the effects of molecular asymmetry, molecular weight, and melting point of the matrix on the esr spectra of oxy radicals.

### Experimental Section

**Materials.** Di-*t*-butyl peroxide, *t*-butyl hydroperoxide, and cumyl hydroperoxide were obtained from Lucidol Co. They were fractionated under reduced pressure, the fraction which contained the theoretical active oxygen content being collected. Dicumyl peroxide is a product of Hercules Inc. Di-*t*-butyl peroxide was purified by passing through a 24-in. column of neutral alumina under a nitrogen atmosphere immediately before use.

Cumene from Eastman Organic Chemicals was fractionated. The preparations of hydroperoxides of squalane, polyethylene, and polypropylene have been described.<sup>6</sup>

Two hindered phenols were used here, 2,6-di-*t*-butyl-*p*-cresol and 1,3,5-tris(3,5-di-*t*-butyl-4-hydroxytolyl)mesitylene, products of Hercules Inc. and Shell Oil Chemicals, Inc., respectively.

**Photolysis Experiments.** Photolysis was carried out in the esr cavity of a Varian spectrometer with a Hanovia LO (Cat. No. 735 A-7) low-pressure Hg resonance lamp placed directly in front of the cavity window. The lamp emits 90% of 2537-A and 10% of 1849-A radiation. Since the latter was found to excite spin centers in the quartz dewar insert, a 2-in.-square quartz plate was attached to the window of the cavity as a filter.

**Thermal Decompositions and Oxidations.** The equipment used to produce and measure oxy radicals at elevated temperatures has been described.<sup>1</sup> The results of radicals detected during autoxidation and thermal decomposition of hydroperoxides are presented here.

**Esr Measurements.** The spectra were recorded after the attainment of stationary conditions. This varies from several minutes to 1 hr in various experiments. The  $g$  values of the oxy radicals were calculated by numerical methods.<sup>7,8</sup> The  $g$  value for diphenylpicrylhydrazyl (DPPH) was taken to be 2.0036, and indicated by a marker in the figures. The radical concentration was calculated by comparison of the first moment of the spectrum with that of a standard DPPH solution. The first moment was computed with the aid of a curve follower and a Bendix G-15 computer.

The peroxy radicals have short spin-lattice relaxation times;<sup>9</sup> their signals are not susceptible to saturation broadening at the microwave power level used in this work.

The results given in the tables of the following sections are averages of two or more measurements. Attainment of stationary conditions was confirmed in many of the photolysis experiments.

### Results

***t*-Butylperoxy Radical.** The *t*-butylperoxy radical was produced *in situ* by vacuum irradiation of a sample of di-*t*-butyl peroxide containing 1% of *t*-butyl hydroperoxide. Oxygen has no apparent effect. At  $-154^\circ$ , the radical was stable. The line width and shape

change with temperature is described below; there is no contact hyperfine structure in any spectrum. Vacuum irradiation of purified di-*t*-butyl peroxide alone gave no esr signal. We concur with the spectral assignment of Ingold and Morton<sup>5</sup> and attribute the spectra to *t*-butyl peroxy radical.

At  $-157^\circ$ , the esr spectrum of  $(\text{CH}_3)_3\text{COO}\cdot$  is an asymmetric singlet; the anisotropic  $g$  values are  $g_{\perp} = 2.0074$  and  $g_{\parallel} = 2.0201$ . The average,  $\bar{g}$ , is 2.0116. The line shape is Gaussian. At  $-106^\circ$ , it becomes difficult to distinguish  $g$  anisotropy. The line shape function appears to be an admixture of Gaussian and Lorentzian. The line width at maximum slope is about 16 gauss. Further increase of temperature causes a narrowing of the line width. The value of  $\bar{g}$  becomes constant at about 2.0120.

At the melting point ( $-42^\circ$ ), the esr spectrum is Lorentzian in shape. The line width is only 9 gauss and it is symmetric. However, the line width was observed to increase continuously with further increase of temperature. The results are given in Table I.

Table I. Esr Spectra of *t*-Butyl Peroxy Radical

Temp, °C	$\bar{g}$	$\Delta\omega$ , gauss	$[(\text{CH}_3)_3\text{COO}\cdot] \times 10^5$ mole l. <sup>-1</sup>
-157	2.0116 <sup>a</sup> { $g_{\perp} = 2.0074$ $g_{\parallel} = 2.0210$ }		1.8
-106	2.0089	16	2.0
-90	2.0108	16	1.9
-70	2.0114	12	1.7
-53	2.0120	10	1.7
-42	2.0212	10	27
-30	2.0120	13	14
-23	2.0123	15	7.4
-17	2.0119	16.5	4.9
-14	2.0113	18	4.6
-5	2.0125	21	3.7
+5	2.0116	25	3.7
+7	2.0127	25	2.9
+20	2.0124	30	2.9
	2.0144 <sup>a</sup>		
	2.0136 <sup>b</sup>		

<sup>a</sup> See ref 5. <sup>b</sup> M. F. R. Mulcahy, J. R. Stevens, and J. C. Ward, *Australian J. Chem.*, **18**, 1177 (1965).

It is interesting to note the changes in the photostationary radical concentrations as a function of temperature, as shown in Figure 1. From  $-157^\circ$  up to the melting point, the concentration was about  $2 \times 10^{-5}$  mole l.<sup>-1</sup> and relatively independent of temperature. Upon melting, the radical concentration increased abruptly. With further increase of temperature, the radical concentration decreases rapidly until a constant level is again attained, about 50% higher than that in the solid state.

**Cumyl Peroxy Radical.** The same radical species ( $g$  values and line width) were obtained by (1) photolysis of dicumyl peroxide in the presence of cumyl hydroperoxide, (2) photolysis of cumyl hydroperoxide alone, and (3) photolysis of cumene saturated with oxygen. Most of the results reported here pertain to radicals generated by the third method. None of the spectra has discernible contact hyperfine structure. Purified dicumyl peroxide was dissolved in cumene and vacuum irradiated. No detectable amount of radicals was ob-

(4) M. C. R. Symons, *Advan. Phys. Org. Chem.* **307** (1963).

(5) K. U. Ingold and J. R. Morton, *J. Am. Chem. Soc.*, **86**, 3400 (1964).

(6) J. C. W. Chien and H. Jabloner, submitted for publication.

(7) M. M. Malley, *J. Mol. Spectry.*, **17**, 210 (1965).

(8) Ya. S. Lebedev, *Zh. Strukt. Khim.*, **4**, 22 (1963).

(9) I. Nitta, S. Ohnishi, Y. Ikeda, and S. Sugimoto, *Ann. Rept. Japan. Assoc. Radiation Res. Polymers*, **2**, 215 (1960).

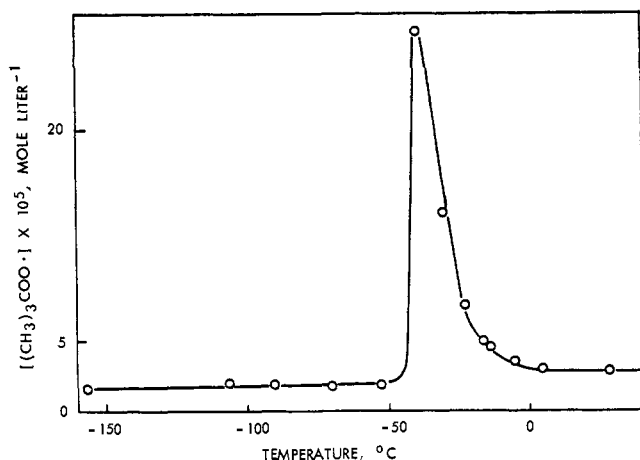


Figure 1. Change of *t*-butyl peroxy radical concentration with temperature and phase.

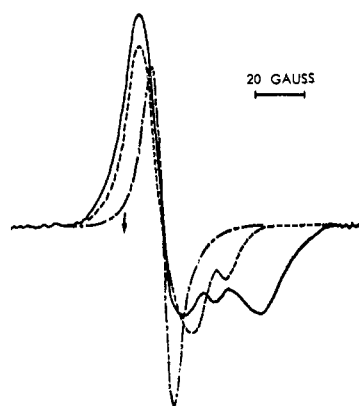


Figure 2. ESR spectra of cumyl peroxy radicals: —,  $-147^\circ$ ; ---,  $-122^\circ$ ; - · - · -,  $-99^\circ$ .

tained over wide temperature ranges. The spectrum reported here is attributed to cumy peroxy radical.

At temperatures lower than  $-129^\circ$ , the esr spectra of cumyl peroxy radical are markedly anisotropic (Figure 2). Partial averaging of  $g$  anisotropy occurred between  $-129$  and  $-122^\circ$ ; nearly complete averaging occurred above  $-105^\circ$ . The narrowest line width and the high-

Table II. ESR Spectra of Cumyl Peroxy Radicals

Temp, $^\circ\text{C}$	$g$ values	$\Delta\omega$ , gauss	$[\text{C}_9\text{H}_{11}\text{OO}\cdot] \times 10^5$ mole l. $^{-1}$
$-147$	$g = 2.0219$ $\left\{ \begin{array}{l} g_{11} = 2.0132 \\ g_{22} = 2.0231 \\ g_{33} = 2.0296 \end{array} \right.$		0.95
$-129$	$g = 2.0210$ $\left\{ \begin{array}{l} g_{11} = 2.0125 \\ g_{22} = 2.0213 \\ g_{33} = 2.0292 \end{array} \right.$		1.0
$-122$	$g = 2.0158$ $\left\{ \begin{array}{l} g_{11} = 2.0140 \\ g_{\perp} = 2.0194 \end{array} \right.$		1.1
$-111$	$g = 2.0182$ $\left\{ \begin{array}{l} g_{11} = 2.0167 \\ g_{\perp} = 2.0212 \end{array} \right.$		1.1
$-105$	$\bar{g} = 2.0177$	13	1.6
$-104$	$\bar{g} = 2.0159$	12	2.4
$-99$	$\bar{g} = 2.0160$	4	5.6
$-97$	$\bar{g} = 2.0157$	2	15.0
$+22$	$\bar{g} = 2.0160$	8	0.31
$+74^a$		10	0.41

<sup>a</sup> J. R. Thomas, *J. Am. Chem. Soc.*, **85**, 591 (1963).

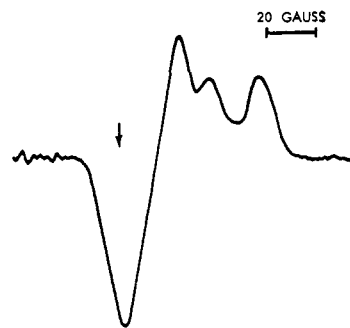


Figure 3. ESR spectrum of polypropylene peroxy radical at  $110^\circ$ .

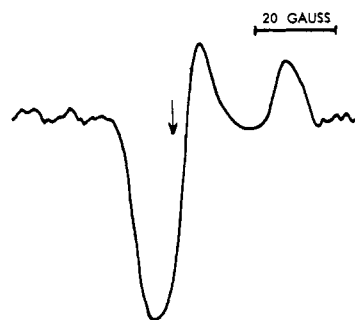


Figure 4. ESR spectrum of polypropylene peroxy radical at  $120^\circ$ .

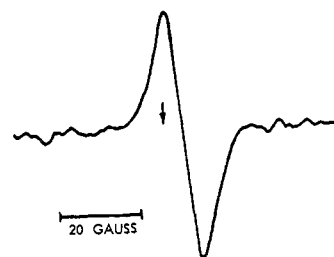


Figure 5. ESR spectrum of polypropylene peroxy radical at  $130^\circ$ .

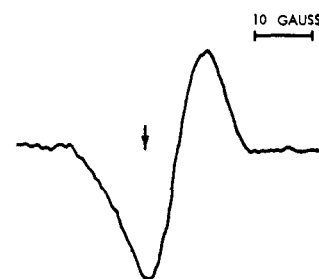


Figure 6. ESR spectrum of polypropylene peroxy radical at  $140^\circ$ .

est radical concentration were again coincident with the melting of the matrix ( $-97^\circ$ ). These results are summarized in Table II.

**Polypropylene Peroxy Radicals.** Several hundred esr spectra of radicals in the autoxidizing polypropylene were recorded. The temperature range covered was  $110$ – $150^\circ$ . Figures 3–6 are typical examples. In general, the spectra at  $110^\circ$  show marked anisotropy independent of the molecular weight or the crystallinity of the polypropylene used. The spectra were unchanged when the sample was quenched to stop the oxidation abruptly. These radicals are indefinitely stable at Dry Ice temperature either in the presence or in the absence

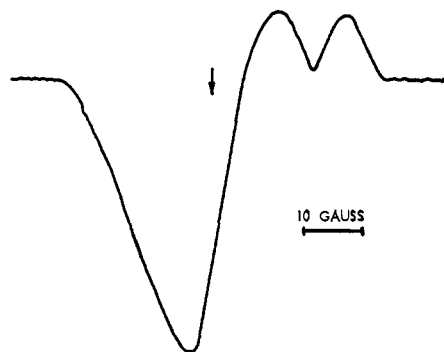


Figure 7. Polyethylene hydroperoxide photolyzed at  $-119^\circ$  *in vacuo*.

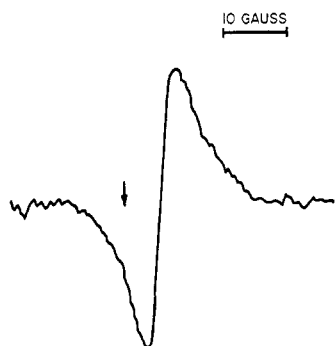


Figure 8. Polyethylene hydroperoxide heated to  $120^\circ$  in the presence of oxygen.

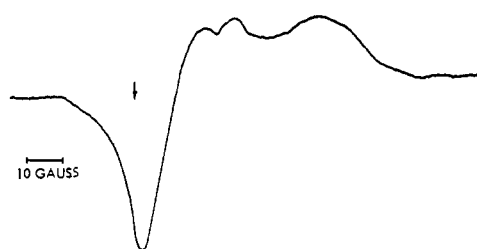


Figure 9. Squalane hydroperoxide photolyzed at  $-100^\circ$ .

of oxygen. The  $g$  values are:  $g_{11} = 2.0135$ ,  $g_{22} = 2.0245$ , and  $g_{33} = 2.0356$ .

At  $120^\circ$ , the spectra showed either partial averaging of  $g$  anisotropy as shown in Figure 4 for crystalline polypropylene (50% crystallinity by X-ray and density measurements) or nearly complete averaging to resemble Figure 5 (amorphous samples). For the former,  $g_{11} = 2.0061$ ,  $g_{\perp} = 2.0187$ .

At  $130^\circ$ , most of the spectra are symmetric; the spectra parameters are:  $\bar{g} = 2.0067$  and  $\Delta\omega = 8.6$  gauss.

At  $140^\circ$ , the symmetric spectra have  $\bar{g} = 2.0067$  and  $\Delta\omega = 7.4$  gauss. At  $150^\circ$ , the line width is about 8 gauss.

The esr spectra of radicals produced by the photolysis of polypropylene hydroperoxide are the same as those described above.

**Other Peroxy Radicals.** Figure 7 shows the spectrum of radicals at  $-119^\circ$  when polyethylene hydroperoxide is photolyzed; Figure 8 is the spectrum when the same compound was thermally decomposed at  $120^\circ$ . The spectra of squalane hydroperoxide photolyzed at  $-100^\circ$

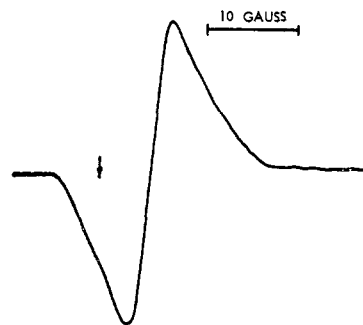


Figure 10. Squalane hydroperoxide photolyzed at  $-51^\circ$ .



Figure 11. ESR spectrum of radical I in polypropylene.

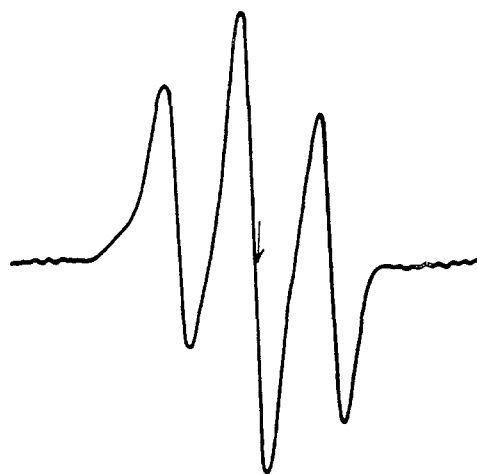


Figure 12. ESR spectrum of radical II in polypropylene.

and  $-51^\circ$  are given in Figures 9 and 10, respectively. The melting point of squalane is  $-80^\circ$ .

**Phenoxy Radicals.** The phenoxy radicals derived from hindered phenols have been described extensively.<sup>10</sup> The two phenols used here are 2,6-di-*t*-butyl-*p*-cresol (I) and 1,3,5-tris(3,5-di-*t*-butyl-4-hydroxytolyl)mesitylene (II). Their spectra were obtained in polypropylene by either the thermal decomposition of polypropylene hydroperoxide containing the phenols or by the thermal oxidation of polypropylene containing these phenols.

The spectrum of I at  $110$ – $140^\circ$  was identical with those obtained from the  $\text{PbO}_2$  oxidation of the parent phe-

(10) (a) J. E. Bennett, *Nature*, **186**, 385 (1960); (b) J. K. Becconsall, S. Clough, and G. Scott, *Trans. Faraday Soc.*, **56**, 459 (1960); (c) N. M. Atherton, E. J. Land, and G. Porter, *ibid.*, **59**, 818 (1967); (d) T. J. Stone and W. A. Waters, *J. Chem. Soc.*, 213, 408, (1964).

not<sup>10b</sup> (Figure 11). All the contact hyperfine structures are clearly resolved. Radical I· is unstable at room temperature.

The spectra of II· at 110–140° is shown in Figure 12. The expected hyperfine structures of three sets of triplets were not resolved. Radical II· is stable in the polypropylene matrix at room temperature.

### Discussion of Results

Photolytic dissociation of pure di-*t*-butyl peroxide gave no detectable esr signal; the spectrum obtained in the presence of *t*-butyl hydroperoxide is attributable to the *t*-butyl peroxy radical. Similarly, photolytic dissociation of pure dicumyl peroxide gave no detectable esr signal; the spectrum obtained in the cumene oxidation is likely that of the cumyl peroxy radical. The radicals observed during oxidations of polypropylene and polyethylene and during the decomposition of hydroperoxides of these polymers are probably also the peroxy radicals. The observed *g* values are comparable to those found for the *t*-butyl and cumyl peroxy radicals.

When a radical with nonzero spin-orbit coupling is rigidly held in a matrix, its spectrum is characterized by the three principal components of the anisotropic *g* tensor, in the absence of any molecular symmetry, and by two *g* values for cylindrical symmetry. Rotation of the groups results in averaging of *g* values. This concept will be used in discussing the averaging of *g* anisotropy with motion and with molecular symmetry.

The results in Table I suggest a cylindrical symmetry for the *t*-butyl peroxy radical at –157°. Apparently, the *t*-butyl group does not inhibit the free rotation<sup>11</sup> of the C–OO bond. At temperatures about 60° below the melting point of the matrix, complete averaging of the *g* values is observed, implying appreciable rotational freedom of the molecule in space. Some dipolar coupling still remained at this temperature, as evidenced by the observed line width. More rapid molecular tumbling, which averages dipolar coupling to zero, probably occurred at 10–20° below the melting point. Usually a faster rate of molecular tumbling is required to average dipolar coupling, the magnitude of which field<sup>12</sup> has a range of about 60 gauss, than what is necessary to average the *g* anisotropy.

The steric effect on *g* averaging is demonstrated by the cumyl peroxy radical. The radical attains cylindrical symmetry only when all the groups are freely rotating. Consequently, anisotropy persists until 30° below the melting point. Complete averaging of *g* values occurs at a slightly higher temperature. Minimum line width of 2 gauss is attained only near the melting point.

The variation of *g* anisotropy of the peroxy radicals of polyethylene and polypropylene with reference to the melting point cannot be considered. These radicals are believed to reside predominantly in the amorphous phase.<sup>13</sup> However, free rotation is hindered by virtue of the size of the group and of the chain entanglement. Evidently extensive rotational freedom is not possible

(11) Since the *g* values differ by less than 1%, rotation is considered to be faster than 10<sup>8</sup> sec<sup>-1</sup>.

(12) A. Abragam, "The Principles of Nuclear Magnetism," Clarendon Press, London, 1961, p 380.

(13) F. H. Winslow and W. L. Hawkins, "Crystalline Olefin Polymers," R. A. V. Raff and K. W. Doak, Ed., Interscience Publishers, Inc., New York, N. Y., 1965, pp 838–840.

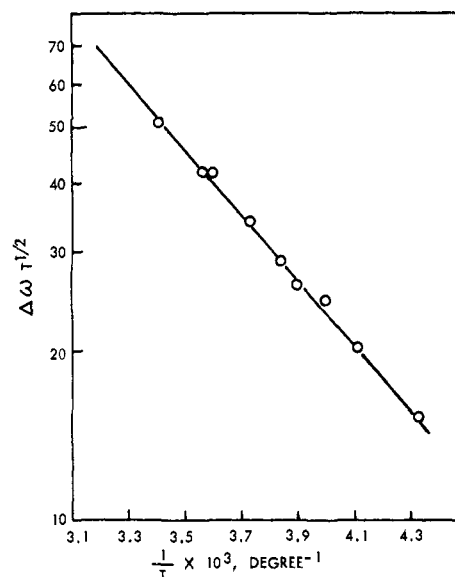


Figure 13. Line width variation with temperature for *t*-butyl peroxy radical.

until the temperature greatly exceeds the second-order transition temperatures. A point of interest is that complete averaging of *g* anisotropy and dipolar coupling appears to occur at the same temperatures.

The motional freedom of the inhibitor molecules can be deduced from the esr spectra of the corresponding phenoxy radicals. The complete resolution of the contact hyperfine structures of radical I· (Figure 11) indicates rapid molecular tumbling. The fact that this radical cannot be stably trapped in polypropylene at room temperature supports this freedom of motion. In contrast, the esr spectra showed that similar molecular tumbling is not possible for radical II·.

The concentrations of *t*-butyl peroxy radical showed large increases near the melting points of the matrices. The photolysis of di-*t*-butyl peroxide yields pairs of *t*-BuO· radical which react with *t*-BuOOH to produce the *t*-BuOO· radicals. The latter reaction could occur only outside the cage if a molecule of *t*-BuOOH is absent within the cage. Furthermore, this reaction has to compete with other reactions of radicals such as combination. The reaction which leads to *t*-BuOO· radical is expected to increase significantly near the melting point of the matrix. The results for cumyl peroxy radical can be similarly accounted for.

The residual line width of  $S = 1/2$  paramagnetic species has been attributed to spin-rotational relaxation.<sup>14</sup> According to this mechanism, the line width is proportional to  $T/\eta$ . Using the Eyring equation for viscosity,<sup>15</sup> the line width should vary with temperature according to  $\Delta\omega \propto T^{-1/2} \exp(-E/RT)$  where *E* is the diffusional activation energy. The results of Table I are plotted accordingly in Figure 13. The linearity obtained suggests that spin relaxation by the spin-rotational process is probably of importance here.<sup>16</sup> The diffusional activation energy of *t*-butyl peroxy radical in liquid di-*t*-butyl peroxide is thus 2.7 kcal mole<sup>-1</sup>.

(14) P. W. Atkins and D. Kivelson, *J. Chem. Phys.*, **44**, 169 (1966).

(15) S. Glasstone, K. J. Laidler, and H. Eyring, "The Theory of Rate Processes," McGraw-Hill Book Co., Inc., New York, N. Y., 1941, p 486.

(16) J. R. Thomas, *J. Am. Chem. Soc.*, **88**, 2064 (1966).